STRESS ANALYSIS OF GREENHOUSE FILM CONSIDERING THE CONTACT BETWEEN THE FILM-TENSIONING STRAP, FILM, AND FRAME

/

考虑压膜线-棚膜-骨架接触的棚膜受力分析

Cunxing WEI[1)], Hengyan XIE[2,*)], Xin ZHENG[2)], Wenbao XU[2)]

[1)] College of Engineering, Heilongjiang Bayi Agricultural University, Daqing 163319 / China

[2)] College of Civil Engineering and Water Conservancy, Heilongjiang Bayi Agricultural University, Daqing 163319 / China

Tel: +86-459-13766785587; E-mail: xiehy555@byau.cn

Corresponding author: Hengyan Xie

DOI: https://doi.org/10.35633/inmateh-77-97

Keywords: *flat-elliptical pipe greenhouse; contact model; sliding and sticking; fluctuating wind; wind-induced vibration responses*

ABSTRACT

Frequent greenhouse collapses under strong wind conditions highlight the limitations of existing structural design methods. Although most previous studies have focused on the stability and load-bearing capacity of greenhouse frames, the dynamic interaction among the greenhouse film, tensioning straps, and structural frame remains insufficiently investigated. This study proposes a novel flat-elliptical pipe plastic greenhouse and derives its mechanical equilibrium equations to analyze the stress behavior of the greenhouse film under wind loading. Using ABAQUS finite element software, an advanced contact model was developed to examine the wind-induced response of the greenhouse system. The results indicate that the structural frame plays a critical role in governing film deformation. In particular, the contact pressure and shear stress between the frame and the film are significantly higher than those between the film and the tensioning straps, underscoring the necessity of explicitly considering contact effects in greenhouse structural design.

摘要

强风荷载下频繁发生的大棚倒塌现象揭示了现有结构设计方法的不足。尽管大多数研究集中在骨架的稳定性和承载能力上，但关于棚膜、压膜线和骨架之间的相互作用仍缺乏深入研究。本研究针对一种新型平椭圆管塑料大棚，推导了其动力平衡方程，以分析棚膜在风荷载下的受力机制。通过 ABAQUS 有限元软件建立了接触模型，系统地分析了棚膜的风致响应。结果表明，骨架在棚膜变形中的作用至关重要，骨架与棚膜之间的接触压力和剪切应力显著高于棚膜与压膜线之间的接触压力，强调了在大棚结构设计中考虑接触效应的重要性。

INTRODUCTION

Plastic greenhouses are pivotal structures in modern controlled-environment agriculture due to their superior thermal insulation properties, lightweight design, and low construction costs. They are widely utilized for the protective cultivation of crops such as vegetables, fruits, and flowers *(Cheng, 2023; Xie, 2025)*. However, in recent years, the frequency of extreme climate events, particularly strong winds and heavy rainfall, has increased, leading to frequent greenhouse collapses and significant economic losses *(Briassoulis, 2016; Uematsu, 2020)*. This phenomenon highlights the limitations of current design methods, which are predominantly based on empirical approaches and lack comprehensive mechanical analysis support when predicting structural responses under wind loads.

Existing research primarily focuses on the stability analysis of greenhouse frame structures and the investigation of their load-bearing capacity limits. For example, *Ren (2019)* used finite element analysis to develop a 20 m span plastic greenhouse frame model and performed loading analysis based on relevant specifications in China and Europe for typical loads.

Cunxing Wei, Ph.D. Eng.; Hengyan Xie, Prof. Ph.D. Eng.; Xin Zheng, Prof. Ph.D. Eng.; Wenbao Xu, Ph.D. Eng.

The study indicated that the greenhouse frame is particularly sensitive to the combined effects of static wind loads and non-uniform snow loads, and its structural safety is mainly influenced by both strength and stiffness. Similarly, researchers such as *Jiang (2020)*, *Wang (2023),* and *Li (2022)* have studied the wind-induced responses of different types of greenhouse frames under fluctuating wind loads, exploring the effects of fluctuating wind on the structural safety of greenhouses, thereby enriching the theoretical system of wind-induced responses in greenhouse structures. *Xie (2025)* employed the arc-length method to perform a nonlinear buckling analysis of the greenhouse frame, evaluating its stability under extreme loads. Currently, an increasing body of literature indicates that membrane structures experience irreversible damage when in contact with cable-membranes *(Xu, 2025; He, 2022)*. This phenomenon imposes higher demands on the safety and stability of membrane structures. Therefore, this study will incorporate the methods and experiences related to cable membrane contact into the stress analysis of membrane structures, applying them to the mechanical analysis of plastic greenhouses in order to enhance the wind resistance of greenhouse designs under extreme climatic conditions.

Despite progress in the study of wind-induced responses of greenhouse frames and covering materials, the coupling mechanisms between the two remain unclear. Existing studies often neglect the nonlinear deformation and contact behavior of the film and film-tensioning straps under wind loads. These factors, which significantly influence the overall structural response, have not been fully considered. As a result, analyses relying on simplified modeling methods are no longer sufficient for the fine-scale assessment of greenhouse structure safety and reliability under extreme climatic conditions. This situation underscores the necessity of conducting detailed numerical modeling, where the film-tensioning straps, film, and frames are studied as a cohesive system.

Failure to account for the contact relationships between the film-tensioning straps and film, as well as between the film and frames, can lead to significant wrinkling and deformation of the film, increasing the risk of damage. Under wind loads, such defects may cause film rupture, resulting in irreversible damage to both the crops inside the greenhouse and the frame structure, thereby posing serious threats to property safety. To enhance the structural safety and durability of greenhouses, there is an urgent need for systematic studies on their wind-induced responses.

Fig. 1 – Flat-elliptical pipe greenhouse

This study focuses on a novel 10 m–span flat-elliptical pipe plastic greenhouse (FEPG) designed for cold regions of Northern China, as shown in Fig. 1. Using ABAQUS finite element software, five frames models are developed, incorporating the contact interactions between the film-tensioning straps, film, and frames. By deriving the overall mechanical equations of the structure, this research will systematically analyze the impact of different interface contact mechanisms on the wind-induced response of the greenhouse film, providing a theoretical basis for the scientific design and optimization of greenhouse structures.

The main contributions of this study are as follows:

(1) Theoretical contribution: Derivation of the mechanical equilibrium equations for the greenhouse film under wind loading, providing insights into the stress mechanisms of the film.

(2) Methodological contribution: Development of a novel ABAQUS-based contact model to simulate the dynamic interaction between the film, tensioning straps, and frame.

(3) Engineering implications: The findings demonstrate the critical role of the frame in film deformation and suggest design improvements to reduce wind-induced failures in greenhouses."

MATERIALS AND METHODS

Wind-induced vibration analysis method considering contact

This section provides a systematical description of the wind-induced analysis method considering contact between the frames, film and film-tensioning straps. When the greenhouse components are regarded as an integrated structural system, the governing equation of structure can be expressed as:

$$Ku = F_w \tag{1}$$

where K is the stiffness matrix of the integrated structure; u is the displacement vector of the structure; F_w is the external wind load vector acting on the integrated structure.

In previous studies, finite element models were often simplified by binding the film-tensioning strap, greenhouse film, and frame into an integrated component. Under this approach, these components were treated as a single element, and only their equivalent stiffness was considered; this simplification is hereafter referred to as the binding model. Under this assumption, the governing equation given in Eq. (1) is applicable. However, in practical engineering applications, the contact conditions among the film-tensioning strap, film, and frame, including adhesion, slippage, and separation, cannot be neglected. To account for these effects, a contact finite element model (hereafter referred to as the contact model) was developed in this study, as shown in Fig. 2(a).

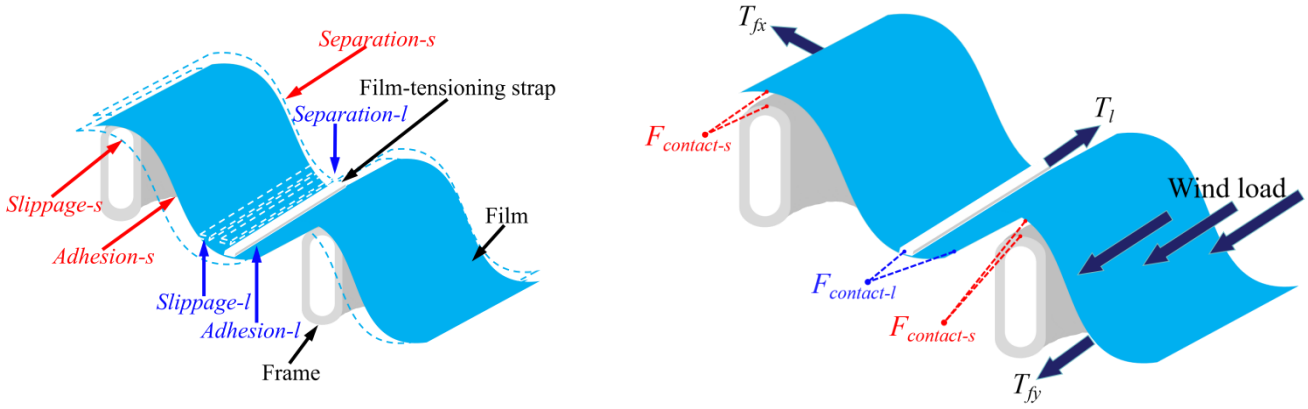

a) Contact conditions of the components *b) Stress conditions of the film*

Fig. 2 – Stress state of the film in practical engineering

As illustrated in Fig. 2(b), when the contact model is employed for wind-induced vibration analysis, an additional contact force must be introduced on the right-hand side of the governing equation to simulate the interactions among the film-tensioning strap, film and frame. Furthermore, due to the prestress in the film and film-tensioning strap, the structure exhibits additional stiffness, as expressed in Eq. (3).

$$K_{total}u = F_w + F_{contact} \tag{2}$$

$$K_{total} = K_0 + K_f + K_l \tag{3}$$

where $F_{contact}$ is the total contact force among the frame, film, and film-tensioning strap; K_{total} is the total stiffness of the structure; K_0 is the original stiffness matrix of the structure, corresponding to the stiffness without considering the prestress; K_f is the stiffness matrix induced by the prestress of the film; K_l is the stiffness matrix arising from the prestress along the compression of the line.

The tangential force equilibrium equation for the film in the structure is as follows:

$$F_{contact} = F_{contact-s} + F_{contact-l} \tag{4}$$

$$F_{contact-s} = \begin{bmatrix} f_n & f_x & f_y \end{bmatrix} \tag{5}$$

where $F_{contact-s}$ is the contact force between the frames and the film, as shown in Fig. 2(b); $F_{contact-l}$ is the contact force between the film-tensioning straps and the film, as also shown in Fig. 2(b); f_n is the normal contact force between two contacting bodies; f_x is the contact force in the x-direction between two contacting bodies; f_y is the contact force in the y-direction between two contacting bodies.

$$f_n = \begin{cases} 0 & when \quad u_n > 0 \\ k_n u_n + \lambda_{i+1} & when \quad u_n \le 0 \end{cases} \tag{6}$$

$$\lambda_{i+1} = \begin{cases} \lambda_{i+1} + k_n u_n & when \quad u_n > \varepsilon \\ \lambda_i & when \quad u_n \le \varepsilon \end{cases} \tag{7}$$

where k_n is the normal contact stiffness; u_n is the contact gap; ε is invasion tolerance; λ_i is the components of Lagrange multipliers of iteration step i for each iteration element.

According to Coulomb's law, three contact states are considered. The first is the separation state, in which the tangential contact force f_x is zero. The second is the sticking state, where the tangential contact force f_x is smaller than the critical friction force. The third is the sliding state, in which the tangential contact force f_x reaches the critical friction force and the film-tensioning straps begins to slide. These three contact states are illustrated in Fig. 2(b). The friction f_x is as follows (f_y is similar):

$$f_x = \begin{cases} k_s u_x & when \quad u_n \le 0 \quad and \quad f = \sqrt{f_x^2 + f_y^2} - \mu f_n < 0 \\ \mu f_n & when \quad u_n \le 0 \quad and \quad f = \sqrt{f_x^2 + f_y^2} - \mu f_n = 0 \\ 0 & when \quad u_n > 0 \end{cases} \tag{8}$$

where k_s is the tangential contact stiffness; u_x is the slip contact distance in the x direction; μ is the coefficient of friction.

Therefore, the governing equation of motion considering the contact between structural components and the prestress in the film-tensioning straps and the film can be expressed as follows:

$$\begin{bmatrix} K_0 & 0 & 0 \\ 0 & K_f & 0 \\ 0 & 0 & K_l \end{bmatrix} \begin{Bmatrix} u_1 \\ u_2 \\ u_3 \end{Bmatrix} = \begin{bmatrix} F_w + F_{contact-s} \\ F_w + F_{contact-s} + F_{contact-l} \\ F_w + F_{contact-l} \end{bmatrix} \tag{9}$$

where, u_1, u_2, u_3 is the displacement vectors of the frame, film and film-tensioning strap.

Finite element model

Material parameter

In this study, the frame is constructed from Q235B galvanized steel pipes, which offer superior strength, rigidity, and corrosion resistance, thereby ensuring adequate support for the film structure under wind loading conditions. The greenhouse film utilized is polyolefin (PO) film, a material widely employed in practical engineering applications. The film-tensioning strap is primarily composed of polyamide (PA), also known as nylon, a high-performance synthetic fiber renowned for its excellent wear resistance and elasticity. The material parameters for each component of the flat-elliptical pipe greenhouse are summarized in Table 1.

Table 1

Material parameters of the frame, film and film-tensioning strap

Material	b×h or R (mm)	t (mm)	ρ (kg/m^3)	f_y (MPa)	λ	E (MPa)
Rafter	30×60	2	7.85	235	0.28	2.1×105
Embedded steel pipe	30×80	2	7.85	235	0.28	2.1×105
Purlin	ϕ20	2	7.85	235	0.28	2.1×105
Film	/	0.12	0.94	/	0.44	500
Film-tensioning strap	20	2	1.15	/	0.35	3500

Contact modal building

In this study, a contact model was developed using ABAQUS finite element software. The structural frame was discretized with C3D8R solid elements, the greenhouse film was modeled with M3D4R membrane elements, and the film-tensioning straps were represented by B31 beam elements.

The C3D8R element is an 8-node hexahedral linear reduced integration element with three degrees of freedom per node. This element effectively mitigates shear locking under bending loads, ensures high accuracy in displacement solutions, and is minimally sensitive to mesh distortion. The M3D4R element is a linear 4-node quadrilateral membrane element specifically designed to simulate thin film structures that only carry in-plane tension, without any bending stiffness. The B31 element is a 2-node linear beam element that is ideal for modeling axial tension or compression, with three degrees of freedom at each node. This element is suitable for modeling hinged connections, as it can only resist axial forces and does not provide bending stiffness, consistent with the assumptions in this study. Given that both the M3D4R and B31 elements are used to model large deformations and geometrically nonlinear behavior, geometric nonlinearity was incorporated into the analysis.

The arch feet are welded to flat-elliptical pipes embedded along the longitudinal axis of the greenhouse, and these pipes are further welded to ground anchors, forming a highly rigid support system. In the ABAQUS model, the connection between the frame feet and the bottom steel pipes is modeled as a fixed boundary, restricting both translational and rotational movement in all directions.

The film, constrained by the frame and film-tensioning straps in practice, is simplified in the model by assuming it is hinged at the bottom, restricting all translational movements. The film-tensioning straps are connected to the ground anchors and modeled as hinged at both ends, with translational movements constrained. The longitudinal tie rods are attached to the frame via clips and are simplified as being bound to the arch rods, with the assumption that the tie rods move in unison with the arches.

The contact pair definition follows the principle that the master surface is typically selected based on its higher rigidity and coarser mesh, while the slave surface is chosen based on its finer mesh. In this study, nodes on the frame are selected to establish point-to-surface contact pairs with the film surface. Similarly, nodes on the film-tensioning strap are selected to establish point-to-surface contact pairs with the film surface.

The calculations and analyses are based on the following assumptions:

(1) Relative sliding between the film, film-tensioning straps, and the frames is permitted, and frictional effects are included in the structural response. The frictional forces at the contact surfaces are governed by Coulomb's friction law. The presence of friction may cause asymmetry in the stiffness during the structural analysis, and to improve the convergence of the calculations, an asymmetric solution scheme is employed.

(2) The film material is modeled as an orthotropic elastic material, with the longitudinal and transverse directions remaining perpendicular throughout the deformation process.

(3) The in-plane bending stiffness of the film material is neglected in the model.

(4) The contact algorithm employs the augmented Lagrangian method, which effectively handles the frictional effects and nonlinear behaviors at the contact interfaces, thereby improving the stability and accuracy of the calculations.

Wind load calculation and application

The plastic greenhouse calculated is located in Jiamusi, Heilongjiang Province, China. According to the Chinese standard *(MOHURD, 2016)*, the design service life of the plastic greenhouse is 10 years, the basic wind pressure in Jiamusi is 0.38 kN/m^2, which is the instantaneous wind speed at 3-second time interval. However, according to the Chinese standard *(MOHURD, 2012)*, the basic wind pressure in Jiamusi is 0.65 kN/m^2 in 50-year return at 10-minute time interval.

According to the Chinese standard *(MOHURD, 2016)*, the ratio of wind pressure in 10-year return to wind pressure in 50-year return is 0.734, therefore the basic wind pressure in 10-year return at 10-minute interval is 0.65×0.734=0.477kN/m^2. The basic wind pressure is 0.477kN/m^2 for the sake of security.

According to the Bernoulli equation in fluid mechanics, the relationship between wind pressure and wind speed is:

$$w = \frac{1}{2}\rho v^2 = \frac{\gamma}{2g}v^2 \tag{10}$$

where: w is wind pressure, kN/m^2; ρ is air density, kPa; v is wind speed, m/s; γ is air gravity density, kN/m^3; g is gravitation acceleration, m/s^2.

In the above equation, the air gravity density ρ is 0.012018kN/m^3 at the standard atmospheric pressure of 101.235 KPa. Jiamusi is located near 45° north latitude, g =9.8m/s^2. Under these conditions, the wind pressure can be calculated using Eq. (10):

$$w = \frac{1}{2}\rho v^2 = \frac{0.012018}{2\times 9.8}v^2 = \frac{v^2}{1630} \tag{11}$$

According to the relationship between wind pressure and wind speed, the mean wind speed is 27.88 m/s under the conditions of a 10 m reference height, terrain category B, a 10-year return period, and a 10-min averaging interval.

In accordance with the *Code for Design Loads of Horticultural Greenhouse Structures (GB/T 51183–2016)*, the wind load acting perpendicular to the greenhouse surface is calculated as follows when analyzing the main greenhouse structure:

$$w_k = \mu_s \mu_z w \tag{12}$$

where: w_k is the standard value of the wind load (kN/m^2); μ_s is the shape coefficient of wind pressure shown in Fig. 3; μ_z is the wind pressure height variation coefficient; w is the wind pressure acting on structure (kN/m^2).

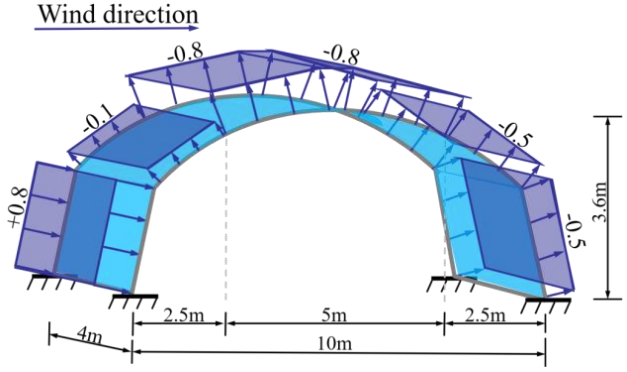

Fig. 3 – Shape coefficient of wind pressure

In this study, the calculated wind load was applied to the film of the flat-elliptical pipe greenhouse as a surface load, and was subsequently transmitted to the frame through the film.

RESULTS AND DISCUSSION

Analysis of contact state

To investigate the contact state between the frames and the film, as well as between the film-tensioning straps and the film under the wind load, this section presents the contact state of these components after model deformation, as illustrated in the Fig. 4.

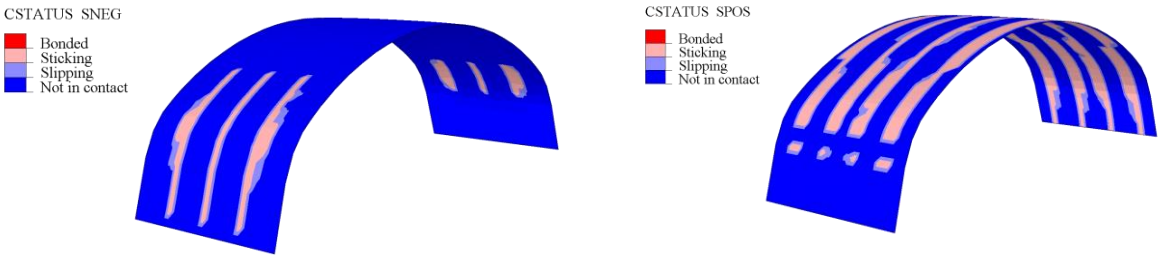

a) Frames-film *b) Film-tensioning straps-film*

Fig. 4 – Contact state

As shown in Fig. 4, the contact regions between the frames and the film are mainly concentrated from the windward foot to the shoulder and at the leeward shoulder. These regions appear as elongated strips. This phenomenon can be attributed to the wind load: the film is pressed against the frames on the windward side due to wind pressure, while suction on the leeward side also causes contact between the film and the frames. Under these conditions, the film exhibits a deformation trend bulging from the windward foot toward the leeward shoulder, which in turn induces contact between the film-tensioning straps and the film. The contact region is primarily located from the windward mid-span to the leeward bottom, further confirming the deformation characteristics of film under wind load observed in practice, which as shown in Fig. 5.

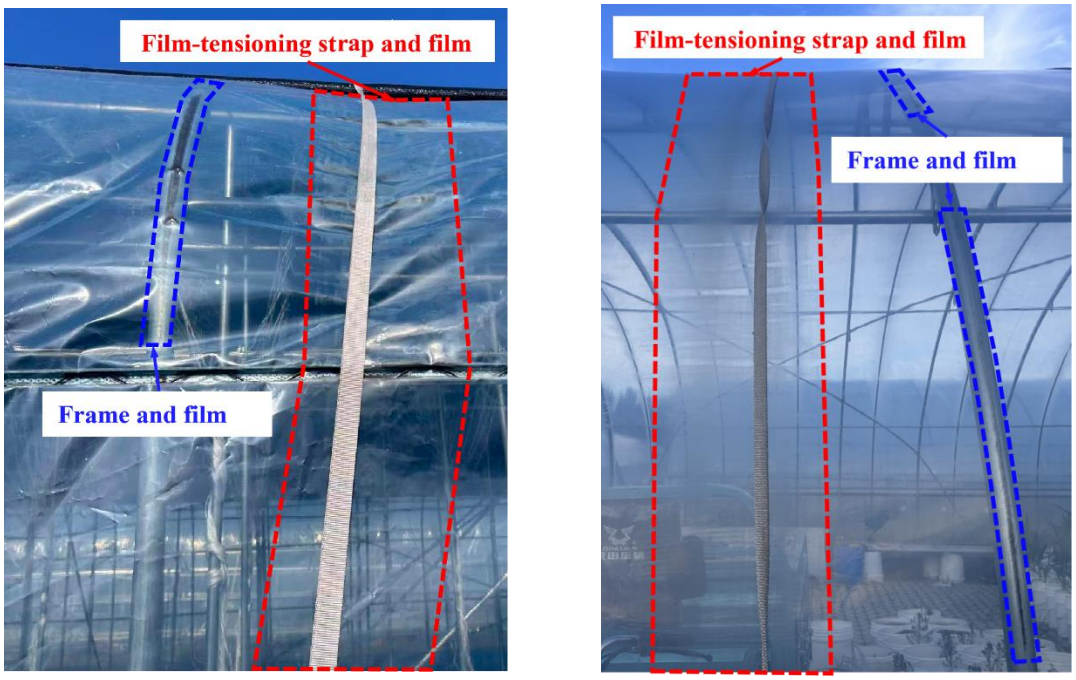

a) Case 1 *b) Case 2*

Fig. 5 – Deformation characteristics of film in practical engineering

In the Fig. 4, the sticking and slipping regions represent adhesion and sliding positions between the film-tensioning straps and the film, respectively. Compared with the contact regions between the frames and the film,

the contact regions between the film-tensioning straps and the film is considerably larger, particularly in the tangential direction, where a significant increase in sliding distance is observed. These results indicate that the full dynamic wind load markedly intensifies the sliding of the film-tensioning straps on the film surface.

Analysis of contact pressure

To investigate the contact pressure between the frames and the film, as well as between the film-tensioning straps and the film under the wind load, this section presents the contact pressure of these components after model deformation, as illustrated in the Fig. 6.

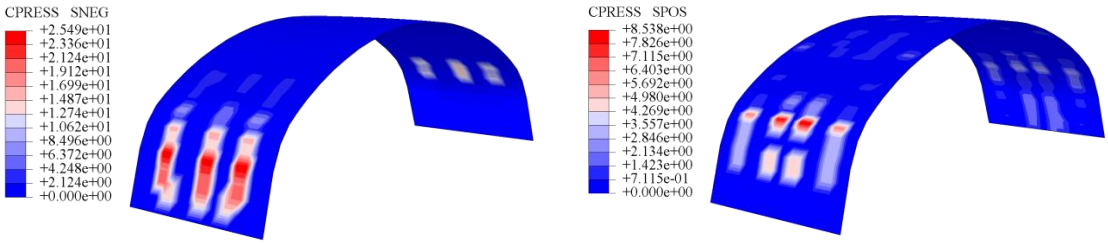

a) Frames-film *b) Film-tensioning straps-film*

Fig. 6 – Contact pressure

As shown in Fig. 6, the contact pressure between the frames and the film is primarily distributed along the windward side of the three main frames, extending from the foot to the shoulder region. The film experiences the greatest stress at the windward mid-span, with a maximum contact pressure of 25.49 Pa. In contrast, the contact pressure between the film-tensioning straps and the film is mainly concentrated along the windward side of the four central film-tensioning straps, from the foot to the mid-span, while the film similarly experiences the highest stress at the windward mid-span. The maximum contact pressure in this case is 8.538 Pa. Notably, the contact pressure between the film-tensioning strap and the film is distributed over a wider area, spanning from the windward foot to the leeward foot. At this time, the maximum contact pressure between the frame and the film is approximately three times that between the film-tensioning straps and the film, indicating that the frames induces a substantially greater radial deformation of the film than the film-tensioning straps. These results are consistent with the radial deformation patterns of greenhouse films observed in practical engineering.

Analysis of shear stress

To investigate the contact shear stress between the frames and the film, as well as between the film-tensioning straps and the film under the wind load, this section presents the contact pressure of these components after model deformation, as illustrated in Fig. 7.

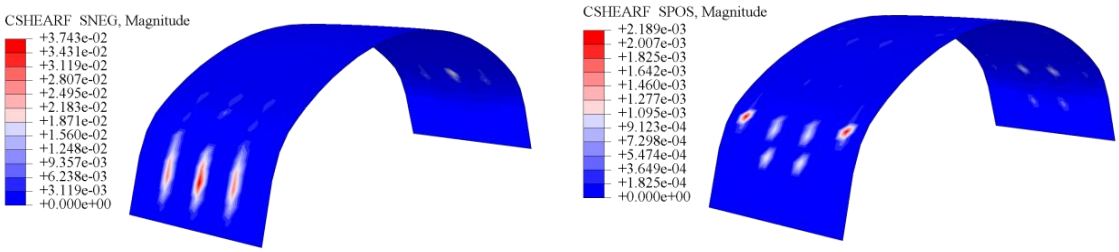

a) Frames-film *b) Film-tensioning straps-film*

Fig. 7 – Contact shear stress

As shown in Fig. 7, under the full dynamic wind load, the contact shear stress between the frames and the film is primarily distributed along the windward side of the three main frames, extending from the foot to the shoulder region. The film experiences the greatest stress at the windward mid-span, with a maximum contact shear stress of 0.03743 Pa. In contrast, the contact shear stress between the film-tensioning straps and the film is mainly concentrated along the windward side of the two central film-tensioning straps, from the foot to the mid-

span, while the film similarly experiences the highest stress at the windward mid-span adjacent to the two lines. The maximum contact shear stress in this case is 0.002189 Pa. Notably, the maximum contact shear stress between the frame and the film is approximately 17 times that between the film-tensioning strap and the film, indicating that the tangential effect of the frame on the film is significantly greater than that of the film-tensioning straps. Consistent with previous studies, the constraint imposed by the film-tensioning straps reduces the tangential sliding of the film, thereby lowering the contact shear stress between the film and the lines.

CONCLUSIONS

This study presents a comprehensive analysis of the wind-induced responses of a novel flat-elliptical pipe plastic greenhouse, with a particular emphasis on the complex interactions between the greenhouse film, film-tensioning straps, and frames under wind loads. Through theoretical derivation, the actual stress conditions of the greenhouse film during wind-induced response are clarified. By developing an advanced contact model using ABAQUS finite element software, the research demonstrates the significant influence of various interface contact mechanisms on the film. The results reveal that, under wind load, the contact pressure and shear stress between the frames and the film are considerably higher than those between the film-tensioning straps and the film. The maximum contact pressure between the frames and the film reaches 25.49 Pa, whereas the contact pressure between the film-tensioning straps and the film is only 8.538 Pa. Similarly, the maximum contact shear stress between the frames and the film is 0.03743 Pa, which is approximately 17 times higher than that between the film-tensioning straps and the film. This study provides new insights into the wind-induced response of a novel flat-elliptical pipe plastic greenhouse. Our findings suggest that the frame plays a critical role in film deformation under wind load and that contact effects must be considered in greenhouse design. Future work will involve parametric studies to optimize greenhouse design parameters and experimental validation to confirm the numerical findings.

ACKNOWLEDGEMENTS

This study is supported by Natural Science Foundation of Heilongjiang Province of China (LH2019E072). All authors are grateful for this support.

REFERENCES

[1] Briassoulis. D., Dougka, G., Dimakogianni, D., Vayas, I., (2016). Analysis of the collapse of a greenhouse with vaulted roof. *Biosystems Engineering*, Vol. 151, pp. 495-509, England. DOI: https://doi.org/10.1016/j.biosystemseng.2016.10.018

[2] Cheng W., Wang Y., Wang C., Wang T., He J., Liu Z., Xu Y., (2023). Study on the variation of thermal environment and photosynthesis characteristics of strawberry in a solar greenhouse, *INMATEH - Agricultural Engineering*, Vol. 70, No. 1, pp. 211-220, Bucharest/Romania. DOI: https://doi.org/10.35633/inmateh-70-21

[3] He Y., Zhu M., Zhao Y., Li X., (2022). Influence of different cable—film connection models on wind-induced responses of an air supported film structure with orthogonal cable net. *Thin-Walled Structures*. England. Vol. 180, No. 109840. DOI: https://doi.org/10.1016/j.tws.2022

[4] Jiang Y., Bai Y., Wang C., Wang Y., Pang X., (2021). Dynamic response analyses of plastic greenhouse structure considering fluctuating wind Load. *Advances in Civil Engineering*. Vol. 2021, pp. 1-13, Egypt. DOI: https://doi.org/10.1155/2021/8886557

[5] Li, X., Wang C., Jiang Y., Bai, Y., (2022). Dynamic response analysis of a whole steel frame solar greenhouse under wind loads. *Scientific reports*, Vol. 12, pp. 1-12, England. DOI: https://doi.org/10.1038/s41598-022-09248-z

[6] MOHURD., (2012). *GB 50009-2012 Load code for the design of building structures.* (建筑结构荷载规范). Beijing, China: China Architecture & Building Press (in Chinese). DOI: https://www.mohurd.gov.cn/gongkai/fdzdgknr/tzgg/201207/20120723_210754.html

[7] MOHURD., (2016). *GB/T 51183-2016 Code for the design load of horticultural greenhouse structures.* （农业温室结构荷载规范）. Beijing, China: China Planning Press (in Chinese) https://www.mohurd.gov.cn/gongkai/zhengce/zhengcefilelib/201702/20170214_230578.html

[8] Ren, J., Wang, J., Guo, S., Li, X., Zheng, K., Zhao, Z., (2019). Finite element analysis of the static properties and stability of a large-span plastic greenhouse. *Computers and Electronics in Agriculture.* Vol. 165, pp. 1-9, England. DOI: https://doi.org/10.1016/j.compag.2019.104957

[9] Uematsu, Y., Takahashi, K., (2020). Collapse and reinforcement of pipe-framed greenhouse under static wind loading. *Journal of Civil Engineering and Architecture*, Vol. 14, pp. 583-594, United States. DOI: https://doi.org/10.17265/1934-7359/2020.11.001

[10] Wang, C., Xu Z., Jiang, Y., Bai, Y., & Wang, T., (2023). Numerical analysis of static and dynamic characteristics of large-span pipe-framed plastic greenhouses. *Biosystems Engineering*, Vol. 232, No. 6, pp. 67-80, England. DOI: https://doi.org/10.1016/j.biosystemseng.2023.06.013

[11] Xie H., Wei C., Zheng X., Xu W., (2025). Stability analysis of flat-elliptical greenhouse frame considering initial geometrical imperfections. *INMATEH - Agricultural Engineering*, Vol. 75, No. 1, pp. 369-379, Bucharest/Romania. DOI: https://doi.org/10.35633/inmateh-76-31

[12] Xie Q., Ren J., (2025). Research on greenhouse planting density of landscape flowers in cold regions based on CFD simulation, *INMATEH - Agricultural Engineering*, Vol. 75, No. 1, pp. 469-479, Bucharest/Romania. DOI: https://doi.org/10.35633/inmateh-75-40

[13] Xu X., Sun X., Shi Z., (2025). Investigation on the wind-induced vibration analysis of air-supported membrane structures considering cable-membrane contact. *Journal of Building Engineering*. Vol. 113506, pp. 1-18, England. DOI: https://doi.org/10.1016/j.jobe.2025.113506